PERGAMON

Phytochemistry 55 (2000) 663–673

PHYTOCHEMISTRY

www.elsevier.com/locate/phytochem

Atranones A–G, from the toxigenic mold *Stachybotrys chartarum*

Simon F. Hinkley, Eugene P. Mazzola, James C. Fettinger, Yiu-Fai Lam, Bruce B. Jarvis *

Department of Chemistry and Biochemistry, Joint Institute for Food Safety and Applied Nutrition (JIFSAN), University of Maryland, College Park, MD 20742, USA

Received 7 January 2000; received in revised form 29 March 2000

Abstract

Atranones A–G have been isolated from the toxigenic fungus *Stachybotrys chartarum*. These compounds contain several unusual features including an enol-lactone as part of a 3,7-dioxabicyclo[3.3.0]octane-2-one ring system fused to an 11-membered ring. Two new dolabellane diterpenes, related in structure to the atranones were also isolated, which suggests a diterpenoid origin for the C_{24} atranones.

Keywords: *Stachybotrys chartarum* (*S. atra*); Diterpenoids; Dolabellanes; Enol lactones

1. Introduction

The filamentous fungus *Stachybotrys chartarum* (Ehrenb. ex Link) Hughes (*S. atra* Corda) (Jong and Davis, 1976) is associated with numerous cases of animal and human toxicoses (Forgacs, 1972; Hintikka, 1978). This mold was first brought to the attention of chemical investigators because of its detrimental effect on livestock (Forgacs, 1972), and it is now becoming more of a concern in human health. An outbreak of idiopathic pulmonary hemosiderosis (IPH) in infants in Cleveland, OH during 1993–1995 has been attributed to unusually high levels of *S. chartarum* and the closely related fungus *Memnoniella echinata* (Etzel et al., 1998; Jarvis et al., 1998). A high percentage of the infants' homes experienced extensive flood damage which provided the suitable growth conditions for these fungi. Since 1993, over 40 cases of IPH have been reported in the Cleveland metropolitan area of which several resulted in fatalities (Dearborn et al., 1999).

One of the key chemical markers for *S. chartarum* is the production of the highly cytotoxic macrocyclic trichothecenes (LD_{50} in mice ~1 mg/kg) (Jarvis, 1991). These compounds are believed to be the principal toxins responsible for the biological activity of this fungus in cases of animal and human stachbotrytoxicosis. Recently, we reported that, in addition to trichothecenes, a series of immunosuppressant spirophenolic benzolactones and lactams are produced at relatively high levels in cultures of *S. chartarum* (Jarvis et al., 1995). As part of our investigation of fungi isolated from the affected Cleveland homes, it became apparent that several strains did not display the expected cytotoxicity nor the usual metabolite profile (Jarvis et al., 1998). During preliminary analysis of a moderately cytotoxic strain of *S. chartarum*, it became clear that several unique metabolites were present (Hinkley et al., 1999). Detailed analysis of several cultures of *S. chartarum* showed that about two-thirds of the cultures produced a series of new compounds that we have named atranones. We reported preliminary data for atranones A–C (Hinkley et al., 1999), and herein, we report details for atranones A–G. Two additional new compounds of the dolabellane diterpenoid class, closely related in structure to the atranones were also isolated. The production, isolation and characterization by spectroscopic and X-ray crystallographic analysis of these nine metabolites are presented.

2. Results

Rice inoculated with *S. chartarum* (Debrecen 5142, S-11) (Jarvis et al., 1986) was held at room temperature (4 weeks) and the majority of the culture (850 g) extracted. The organic extract was triturated with hexane and chromatographed over polyethyleneimine silica gel (Jarvis,

* Corresponding author. Tel.: +1-301-405-1843; fax: +1-301-314-9121.

E-mail address: bj6@umail.umd.edu (B.B. Jarvis).

0031-9422/00/$ - see front matter
PII: S0031-9422(00)00231-4

1992) to give a fraction containing atranones A–C (**1–3**). These compounds exhibit distinctive orange spots upon TLC development with vanillin spray. Atranone B was separated from A and C by radial chromatography while the latter two required reverse-phase HPLC for complete resolution. Later fractions from the PEI column were subjected to successive radial chromatography yielding atranones D–G (**4–7**) as well as the dolabellanes **8** and **9**.

The structures of atranones A–C (**1–3**) were given in an earlier publication, and their ^{1}H and ^{13}C NMR spectral data are reported therein (Hinkley et al., 1999). In brief, the structures of **1–3** were solved by a combination of spectral techniques (IR, UV, HR–MS, and NMR), including detailed analyses of COSY and HMBC spectra (see Fig. 1) and NOESY (see Fig. 2) of atranone A (**1**). However, even with these techniques, we were unable to determine whether the bicyclo[3.3.0] western portion of the molecule was fused as shown in **1–3**, or was in fact reversed, as shown in **1a**. No 3-bond coupling (HMBC) could be seen between H-7 and C-22. Fortunately, atranone C (**3**) gave a crystal suitable for X-ray crystallographic analysis. These diffraction data decided the issue in favor of the enol lactone system (Fig. 3). The details of the X-ray crystal data for atranone C (**3**) are given in the Experimental.

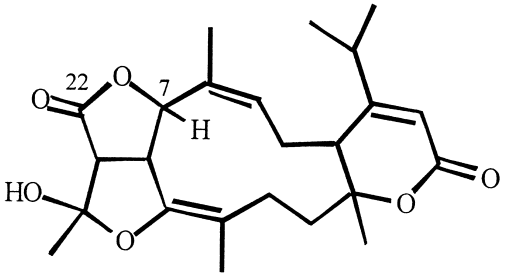

1a

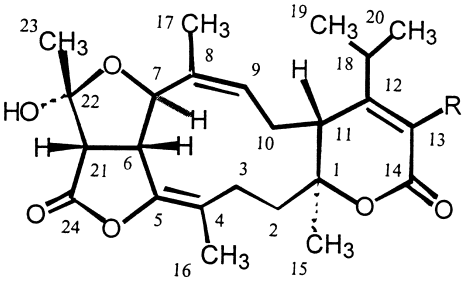

1: R = H
2: R = OMe

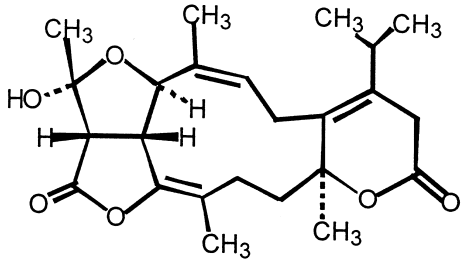

3

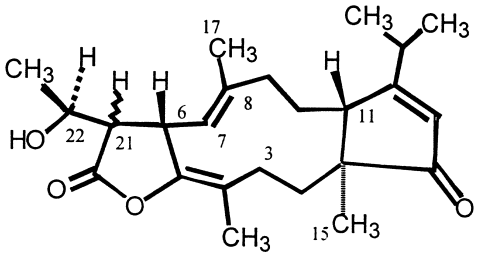

4: H-21 β
5: H-21 α

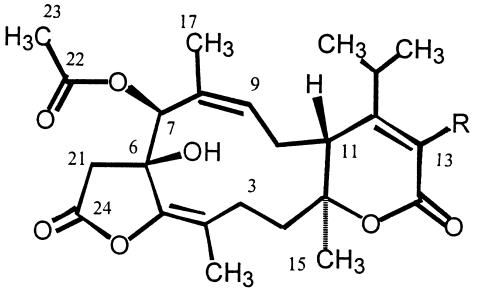

6: R = H
7: R = OMe

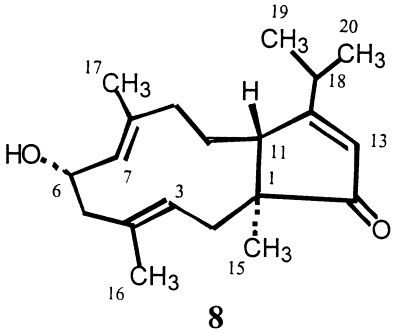

8

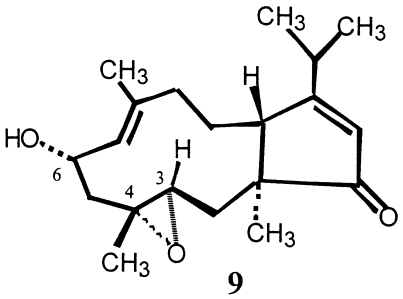

9

Upon further investigation of the more polar constituents from the crude extract, two further unusual metabolites were isolated. Comparison of their spectral data to those of atranones **1–3** indicated they are closely related. Atranone D (**4**) displayed HREI-MS data consistent with molecular formula $C_{24}H_{34}O_4$, requiring 8 degrees of unsaturation. The IR spectrum of **4** indicated two different carbonyl groups (1780, 1693 cm^{-1}), while two further double bonds of similar functionalization to those in **1–3** were clear from analysis of the NMR data (Table 1; ^{13}C: δ 126.7, 137.3 and 114.5, 144.9: C-7, C-8, C-4 and C-5, respectively). Additional unsaturation is present as evidenced by a distinctive set of low-field signals: ^{13}C: δ 212.0, 188.0, 124.3; ^{1}H: δ 5.83. The UV absorption observed (λ_{max} 231 nm, log ϵ 4.17) suggested the aforementioned low-field resonances constituted an α,β-unsaturated group. In view of the five double bonds in **4**, the molecule is tricyclic.

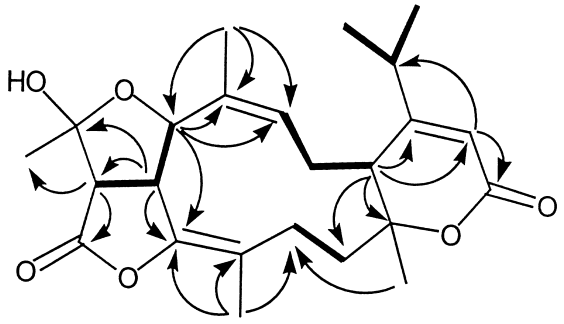

Fig. 1. Key COSY (bold lines) and HMBC (arrows) correlations for atranone A (**1**).

A comparison of the NMR spectral data of atranone D with those of the previous atranones shows several key differences. The lack of a resonance at ~5.2 ppm in the ^{1}H NMR spectrum suggested that the hemiketal ring had changed, while the lactone carbon signal at *ca.* 165 ppm (C-14) in atranones A–C had shifted dramatically downfield to 212.0 ppm. Analysis of HMQC, COSY and HMBC data determined the structure of this more polar atranone to be **4**. One set of key HMBC correlations in atranone D (**4**) was from the H-11, H-15 and H-2 protons to C-14 (212.0 ppm), which completes the cyclopentenone ring. With disassembly of the hemiketal ring without disruption of the conjugated γ-lactone in **4**, we could now confirm the arrangement of the western portion of the molecule, i. e. discard substructures such as **1a** for atranones A–C. This assignment had eluded us until the X-ray analysis of the crystal of atranone C.

Atranone E (**5**) is clearly isomeric with **4**. A comparison of the ^{13}C NMR spectral data for these two metabolites shows no more than a 0.2 ppm difference in resonance frequencies, with the exceptions the alkene groups of the 11-membered ring and carbons C-6, C-21, and C-27 (Table 1). Closer examination and comparison of the proton resonances suggested that a stereochemical difference occurs about the C-6 and/or C-21 centers. Analysis of the 2-D NMR data for **5** confirmed that the base structure is identical to that of **4**, and so the relative stereochemistry of **4** and **5** was compared

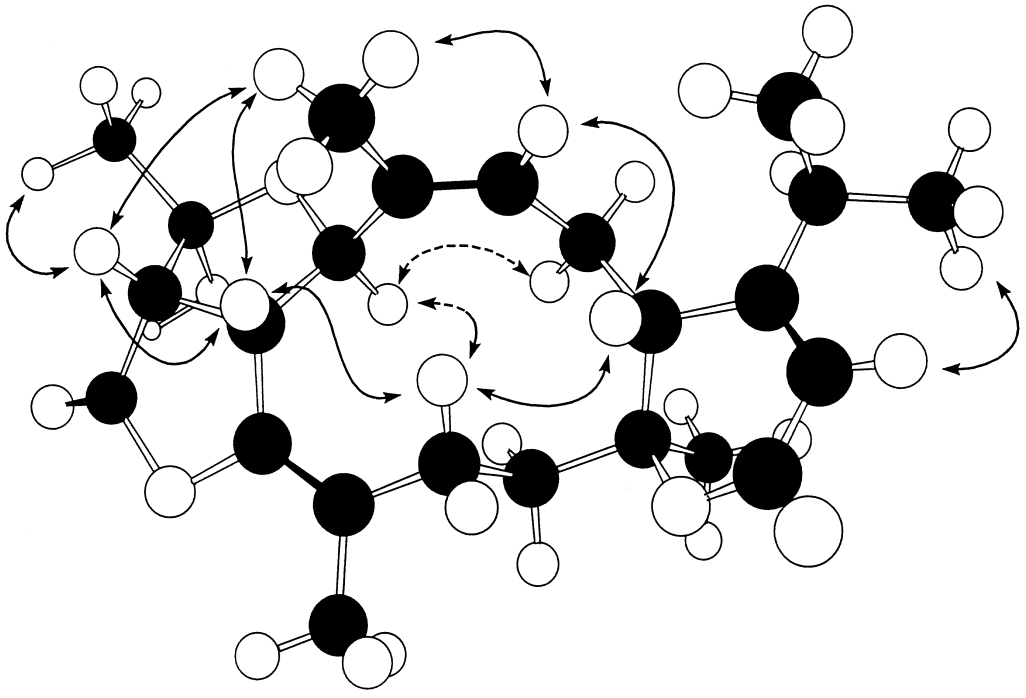

Fig. 2. NOE correlations for atranone A (**1**): solid lines, β; dashed lines, α.

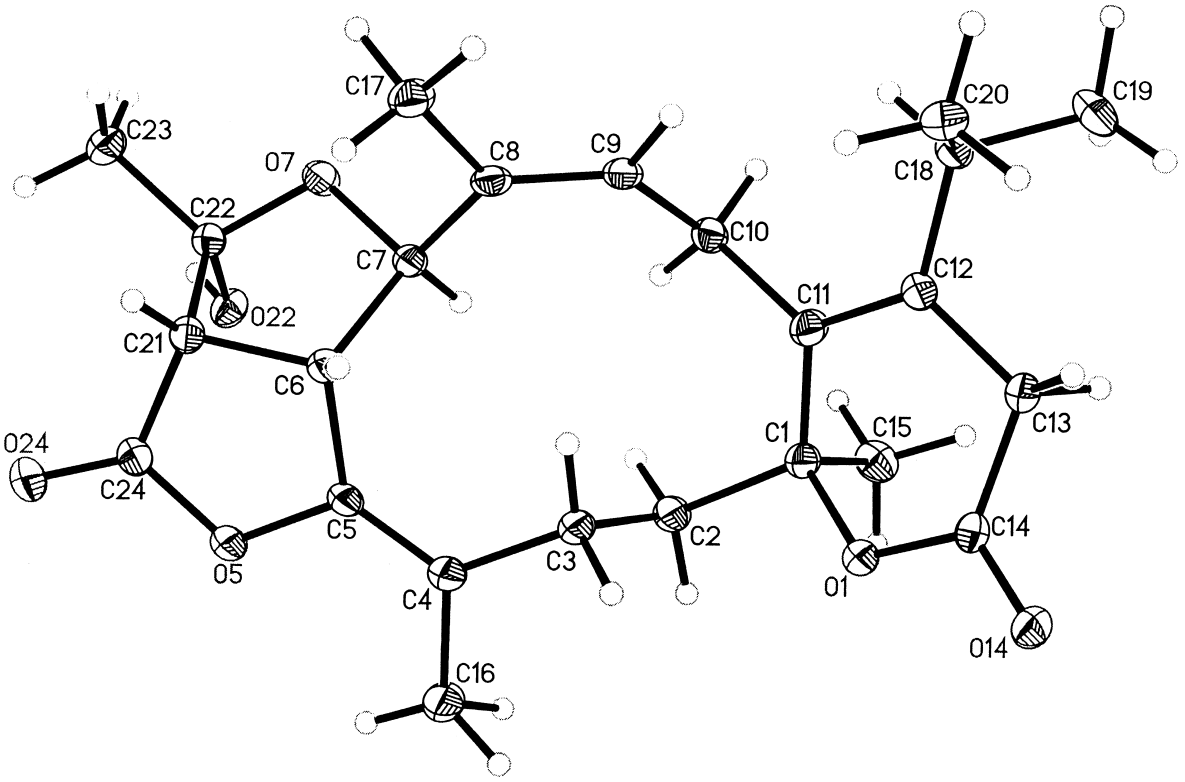

Fig. 3. Molecular plot of atranone C with atoms drawn at their 30% probability ellipsoids; hydrogen atom labels omitted for clarity.

Table 1
^{13}C NMR spectroscopic data for atranones D–G (**4**–**7**)[a]

No.	D (**4**)	E (**5**)	F (**6**)	G (**7**)
1	52.0 (*s*)	52.0 (*s*)	86.4 (*s*)	85.7 (*s*)
2	35.7 (*t*)	35.8 (*t*)	37.4 (*t*)	37.2 (*t*)
3	27.0 (*t*)	27.0 (*t*)	23.6 (*t*)	23.5 (*t*)
4	114.5 (*s*)	115.6 (*s*)	117.0 (*s*)	116.5 (*s*)
5	144.9 (*s*)	143.6 (*s*)	149.5 (*s*)	149.7 (*s*)
6	38.1 (*d*)	39.6 (*d*)	76.5 (*s*)	76.1 (*s*)
7	126.7 (*d*)	129.6 (*d*)	75.2 (*d*)	75.4 (*d*)
8	137.3 (*s*)	135.0 (*s*)	132.6 (*s*)	132.6 (*s*)
9	36.3 (*t*)	36.4 (*t*)	134.0 (*d*)	134.3 (*d*)
10	24.0[b] (*t*)	23.9 (*t*)	25.7 (*t*)	26.1 (*t*)
11	43.7 (*d*)	43.6 (*d*)	43.9 (*d*)	44.5 (*d*)
12	188.0 (*s*)	188.0 (*s*)	169.1 (*s*)	147.1 (*s*)
13	124.3 (*d*)	124.2 (*d*)	112.6 (*d*)	141.0 (*s*)
14	212.0 (*s*)	212.0 (*s*)	165.0 (*s*)	161.1 (*s*)
15	24.0[b] (*q*)	24.2 (*q*)	21.8 (*q*)	21.3 (*q*)
16	15.8 (*q*)	15.5 (*q*)	16.9 (*q*)	16.5 (*q*)
17	16.6 (*q*)	17.0 (*q*)	18.9 (*q*)	20.6 (*q*)
18	29.1 (*d*)	29.1 (*d*)	31.0 (*d*)	30.3 (*d*)
19	21.2 (*q*)	21.2 (*q*)	20.6 (*q*)	20.3 (*q*)
20	22.1 (*q*)	22.1 (*q*)	23.7 (*q*)	20.8 (*q*)
21	50.5 (*d*)	52.9 (*d*)	41.0 (*t*)	40.9 (*t*)
22	66.8 (*d*)	67.5 (*d*)	169.7 (*s*)	169.7 (*s*)
23	20.9 (*q*)	20.8 (*q*)	20.7 (*q*)	20.6 (*q*)
24	175.3 (*s*)	175.6 (*s*)	170.9 (*s*)	171.0 (*s*)
25				59.4 (*q*)

[a] Data recorded at 100 MHz referenced to the solvent peak (δ 77.1 $CDCl_3$). Carbon multiplicity determined by DEPT experiment.

[b] DEPT and HMQC experiments verified the overlap of these signals.

using NOESY experiments. Several points had to be determined: the stereochemistry of the C-1/C-11 ring junction, the orientation of the trisubstituted double bond at the 8,9-position, and the stereochemical relationship between **4** and **5**.

NOESY spectra for **4** showed a strong cross-peak from the H-21 resonance (δ 3.03) to H-6 (δ 4.15) which indicates a *cis*-arrangement for these hydrogens. An E-trisubstituted 7,8-double bond was inferred as no NOE was recorded from the H-7 proton (δ 5.51), to the 17-methyl group (δ 1.72). Although the lack of an NOE is not strong stereochemical evidence (Sanders and Mersh, 1982; Neuhaus and Williamson, 1989), the observed NOE from H-6 to the 17-methyl group resonating at δ 1.72, without an enhancement of the H-7 proton signal (δ 5.51) is possible only with an *E*-configuration for this alkene. The *trans* ring junction for the cyclopentenone system was inferred from the lack of an NOE between the H-11 proton (δ 2.70) and the 15-methyl group (δ 1.01). Further evidence was provided by the series of β-face NOEs recorded between the aforementioned H-11, H-17, H-3b (δ 1.84) and H-6 (δ 4.15); while on the α-face of the large ring, NOEs involving H-7 (δ 5.51), the H-2 protons (δ 1.27, 2.31) and the 15-methyl group (δ 1.01) confirmed that H-11 and the 15-methyl must be in a *trans* configuration.

The NOESY cross peaks for **5**, in comparison to those observed for **4**, indicated that **4** and **5** have very

similar relative stereochemistries. The most significant difference was the lack of an NOE from H-21 (δ 2.50) to H-6 (δ 3.82) in **5** and the observation of an NOE from H-21 to the alkene proton H-7 (δ 5.44). This clearly indicates that the lactone methine hydrogens, H-6 and H-21, are of *trans* orientation, rather than *cis* as observed in all the other atranones. This is consistent with the observed differences in the NMR spectral data at H-21 for these two compounds (Table 2).

The relative stereochemistry of the secondary alcohol moiety at C-22 in **4** and **5** was assessed by comparing NOESY and single frequency NOE experimental results with conformational data provided by molecular modeling experiments. Additional information was provided by comparing proton ^3J coupling constants with those generated by the modified Karplus parameters from the MacroModel software. For both **4** and **5**, a 22-(S*) orientation better satisfied the spectral and modeling data than did a 22-(R*) configuration. Therefore, we assign the relative stereochemistry for atranone D (**4**) as 1S*, 4E, 6R*, 7E, 11R*, 21S* with a tentative assignment of 22S*. Similarly, the assignment 1S*, 4E, 6R*, 7E, 11R*, 21R*, 22S* may be conferred to atranone E (**5**).

Atranone F (**6**) analyzed for $C_{24}H_{32}O_7$ by HREI–MS. ^1H NMR spectral data (Table 2) indicated an acetate group (δ 2.02, 3H, s) as well as a peak consistent with the δ-lactone (δ 5.79), previously encountered in atranone A. DEPT and HMQC experiments gave rise to the molecular formula $C_{24}H_{31}$, suggesting one exchangeable proton, observed in the IR spectrum as a hydroxyl (3390 cm^{-1}). Full 2-D NMR analysis revealed the base structure as depicted in **6**. The connection of the acetate to position 7 was dictated by the chemical shift of C-7 (δ 75.2) as well as a through-oxygen HMBC correlation from H-7 (δ 6.08) to the acetate carbonyl C-22 (δ 169.7). The remaining valence on the C-6 quaternary carbon (δ 76.5) must accommodate the hydroxyl functionality.

Atranone G (**7**) was characterized as the 13-OMe derivative of atranone F (**6**). Structure elucidation was completed using the aforementioned NMR spectroscopic techniques, and by comparison of the ^{13}C NMR data of **6** and **7** (Table 1), which are reminiscent of the differences seen in the ^{13}C NMR data of **1** and **2** (Hinkley et al., 1999). The relative stereochemistry of **7** was ascertained via interpretation of a NOESY experiment. Through-space connectivity was not observed between H-11 (δ 3.26) and the 15-methyl protons (δ 1.36), indicating they are in a *trans* orientation as found in all the atranones. The trisubstituted double bond must be *cis* (Z) due to a NOESY correlation from H-17 (δ 1.76) to H-9 (δ 5.80). Strong NOE correlations involving the H-7 (δ 6.05), H-3a (δ 2.10) and H-10b (δ 2.70) resonances indicate that H-7 projects into the 11-membered ring. A similar series of NOEs involving the H-7 resonance in the center of the large ring was observed in atranones A and B (see Fig. 2). Assigning the stereochemistry of the C-6 hydroxyl required detailed examination of the NOESY data and models. The key strong

Table 2
^1H NMR spectroscopic data for atranones D–G (**4**–**7**)[a]

No.	D (**4**)	E (**5**)	F (**6**)	G (**7**)
2a	1.27 *m*	1.35 *m*	2.00 *m*	1.97 *ddd* 13.4, 11, 8
2b	2.31 *m*	2.34 *ddd* 13.4, 12.8, 5.5	3.24 *dd* 11.4, 11.0	3.22 *dd* 13.4, 11.8
3a	1.30 *m*	1.21 *m*	2.14 *m*	2.10 *dd* 15.1, 11
3b	1.84 *m*	1.99 *ddd* 12.8, 12.2, 2.1	2.34 *m*	2.24 *ddd* 15.1, 11.8, 8
6	4.15 *br dd* 11.5,10.4	3.82 *br dd* 9.5, 8.9		
7	5.51 *br d* 10.4	5.44 *d* 9.5	6.08 *d* 1	6.05 *s*
9a	2.42 *m*	2.40 *m*	5.83 *br* t 8.4	5.80 *dd* 8.1, 8.0
9b	2.22 *dddd* 12.4,12.4, 5.9, 3.0	2.23 m	–	–
10a	1.69 *m*	1.69 *m*	1.87 *m*	1.87 *dd* 15.5, 8.0
10b	2.24 *m*	2.24 *ddd* 13.1,12.9, 4.5	2.74 *m*	2.70 *m*
11	2.70 *dd* 12.2, 1.0	2.70 *br d* 12.9	3.27 *dd* 9.2, 2.2	3.26 *br d* 9.0
13a	5.83 *d* 1.0	5.82 *br s*	5.79 *s*	–
13b	–	–	–	–
15	1.01 3H *br s*	1.10 3H *s*	1.31 3H *s*	1.36 3H *s*
16	1.80 3H *s*	1.80 3H *s*	1.75 3H *s*	1.73 3H *s*
17	1.72 3H *br s*	1.71 3H *d* 2	1.77 3H *br s*	1.76 3H *s*
18	2.62 qq 6.9, 6.7	2.62 *qq* 6.8, 6.7	2.62 *qq* 6.6, 6.7	2.49 *br qq* 6.9, 6.9
19	1.16 3H *d* 6.7	1.16 3H *d* 6.7	1.18 3H *d* 6.6	1.21 3H *d* 6.9
20	1.14 3H *d* 6.9	1.14 3H *d* 6.8	1.06 3H *d* 6.7	1.31 3H *d* 6.9
21a21b	3.03 *dd* 11.5, 5.2-	2.50 *dd* 8.9, 6.3-	2.71 1H *d* 18.13.43 1H *d* 18.1	2.74 *d* 18.03.45 *d* 18.0
22	4.07 *dq* 6.4, 5.2	4.00 *dq* 6.4, 6.3	–	–
23	1.32 3H *d* 6.4	1.30 3H *d* 6.4	2.02 3H *s*	2.01 3H *s*
25	–	–	–	3.67 3H *s*

[a] Data recorded at 500 MHz referenced to the residual solvent peak (δ 7.05 C_6D_6; δ 7.24 $CDCl_3$). Coupling constants in Hz. Each signal integrates for one proton unless specified otherwise.

correlations involving H-7, H-10, and H-3 were best satisfied by a ring geometry with the C-6 hydroxyl group β. Furthermore, this relative stereochemistry is consistent with the NOE observed from H-17 (δ 1.76) to only one of the H-21 methylene resonances (δ 3.45). Models with an α-face hydroxyl, while keeping a conformation that attempts to satisfy all other observed NOEs, forced the 17-methyl into an arrangement less suitable for enhancing only one of the H-21 methylene protons. With a C-6 bearing an α-hydroxyl, models indicate that H-7 and one of the H-2 protons are in very close proximity. However, no strong NOE was observed for this interaction.

Atranone F (**6**) had NOE data complementary to that recorded for **7** indicating the same relative stereochemistry, a result consistent with the very similar ^{13}C NMR spectral data (Table 1). It was anticipated that methylation of the alcohol would provide a derivative that could aid in the stereochemical assignment. Unfortunately, both atranones F and G were unstable and decomposed into multiple unidentified derivatives upon storage before the reaction could be attempted. However, the stereochemical data did define the ring and relative stereochemistry for **6** and **7**, and we assign them as 1S*, 6S*, 7S*, 11R* for both atranones F and G.

The final two compounds isolated from the crude extract of *S. chartarum* were the most easily identified structures, due principally to the extensive analysis of atranones A–G. The less polar of the two, compound **8**, was isolated from combined Chromatotron fractions and analyzed by HREI–MS for $C_{20}H_{30}O_2$. Consideration of the ^{13}C NMR spectroscopic data (Table 3) suggested three unsaturated groups, two olefinic (δ 126.0, 132.5, 134.2, 135.6) and a moiety reminiscent of the cyclopentenone group as found in **4** and **5** (δ 123.8, 190.6, 213.8). This similarity was reinforced by UV data (λ_{max} 236 nm, log ε 3.94) and a strong absorption for a conjugated carbonyl resonance in the IR spectrum (1690 cm^{-1}). This leaves two degrees of unsaturation and indicated that we were now dealing with a bicyclic compound. Since **8** is a C_{20} compound with spectral data closely resembling those of atranones **4** and **5**, an obvious possibility is that **8** belongs to the dipenoid class of dolabellanes (Rodríguez et al., 1998) from whence the atranones could be derived biosynthetically. The structure **8** is proposed based on spectral similarities to the tricyclic atranones (see above) and the bicyclic dolabellanes (Rodríguez et al., 1998), and NMR spectroscopy (HMQC, HMBC and COSY) confirmed this assignment. A NOESY experiment was able to

Table 3
NMR spectroscopic data for dolabellanes **8** and **9**[a]

	8		**9**	
No.	^{13}C	^{1}H HMQC	^{13}C	^{1}H HMQC
1	53.7 (*s*)		50.4 (*s*)	
2a	38.5 (*t*)	1.89 2H *d* 8.3	39.1 (*t*)	0.93 1H *dd* 14.0, 11.1
2b				1.96 1H *m*
3	126.0 (*d*)	5.31 *t* 8.3	62.7 (*d*)	2.97 *dd* 11.1, 1.5
4	134.2 (*s*)		60.1 (*s*)	
5a	48.9 (*t*)	2.08 *dd* 10.3, 9.8	47.3 (*t*)	2.55 *m*
5b		2.58 *dd* 9.8, 5.0		1.23 *m*
6	66.5 (*d*)	4.62 *ddd* 10.3, 10.1, 5.0	65.6 (*d*)	4.58 *ddd* 10.4, 10.3, 5.2
7	132.5 (*d*)	5.10 *d* 10.1	130.5 (*d*)	5.28 *d* 10.3
8	135.6 (*s*)		137.1 (*s*)	
9a	37.6 (*t*)	2.18 *ddd* 12.0, 5.4, 3.0	37.4 (*t*)	2.26 *br dd* 12.9, 5.6
9b		2.34 *m*		2.42 *dd* 12.9, 5.6
10a	27.9 (*t*)	1.34 *dddd* 14.9, 9.5, 5.4, 3.5	27.7 (*t*)	1.36 *m*
10b		1.83 *dddd* 14.9, 12.0, 3.0, 3.0		1.93 *m*
11	47.7 (*d*)	2.34 *m*	48.2 (*d*)	2.38 *br d* 8.5
12	190.6 (*s*)		190.1 (*s*)	
13	123.8 (*d*)	5.84 *s*	123.8 (*d*)	5.85 *s*
14	213.8 (*s*)		212.8 (*s*)	
15	15.7 (*q*)	1.18 3H *s*	15.7 (*q*)	1.30 3H *s*
16	17.2 (*q*)	1.50 3H *s*	17.4 (*q*)	1.13 3H *s*
17	16.2 (*q*)	1.69 3H *s*	16.2 (*q*)	1.79 3H *s*
18	29.6 (*d*)	2.54 *qq* 6.9, 6.8	29.7 (*d*)	2.54 *m*
19	21.4 (*q*)	1.19 3H *d* 6.8	21.3 (*q*)	1.20 3H *d* 6.7
20	22.5 (*q*)	1.10 3H *d* 6.9	22.5 (*q*)	1.06 3H *d* 6.9

[a] Data recorded in $CDCl_3$ at 500 MHz (^{1}H) and 100 MHz (^{13}C) referenced to the relevant solvent signal (^{1}H δ 7.24; ^{13}C δ 77.1). Carbon multiplicity determined by DEPT experiments. Proton resonances integrate for one proton unless specified otherwise.

confirm that the C-1/C-11 bridgehead arrangement is *trans*, as well as define the conformation of the large ring, the configurations of the alkenes, and the stereochemistry of the C-6 alcohol. An unambiguous series of β-face NOE correlations oriented the vinylic methyl groups, H-11 and H-6 methines, as well as H-5a (δ 2.08). Consistently, NOEs were observed from both the H-7 and H-3 to H-5b (δ 2.58). This ring geometry was in complete agreement with the lowest-energy conformation uncovered by our molecular modeling and is consistent with literature findings for the favored conformation of the dolabelladiene 11-membered ring (Shin and Fenical, 1991; Corey and Kania, 1998). Furthermore, calculated coupling constants are again in good agreement with observed data about the C-6 stereocenter. We, therefore, assign the structure as 6α-hydroxydolabella-3*E*,7*E*,12-trien-14-one (**8**).

The similarity in structure between the final new metabolite **9** and dolabellane **8** is evident from the ^{13}C NMR spectroscopic data (Table 3). By inspection, it is not unreasonable to assume epoxidation of the C-3 alkene has resulted; such epoxidation (especially at C-3) is common in dolabellane natural products (Asakawa, 1995; Rodríguez et al., 1997). An epoxide group is consistent with the HREI-MS result that indicated one more oxygen is present in **9** than is found in **8**. The structure (1S*, 3R*, 4R*, 6S*, 11S*)-3,4-epoxy-6-hydroxydolabella-7*E*,12-dien-14-one (**9**) is apparent after analysis of the results from HMQC, HMBC and COSY experiments had been analyzed. NOESY data revealed that a ring conformation of **9** in solution was similar to that of **8**, with the H-15 (δ 1.30), H-7 (δ 5.28), H-3 (δ 2.97) and H-5b (δ 1.23) protons residing on the α-face of the molecule. Correlations on the β-face positioned together the 16- and 17-methyls (δ 1.13 and δ 1.79, respectively), H-5a (δ 2.55), H-11 (δ 2.38), and H-6 (δ 4.58).

3. Discussion

Following the isolation of atranones A–C (**1–3**), we carried out a substructure search for natural products that contained one or more of the atranone A–C structural elements: α,β-unsaturated δ-lactone with an isopropyl substituent at the β-position, an eleven-membered carbocyclic ring, and a 3,7-dioxabicyclo[3.3.0]octane-2-one ring system. Of these three principal substructural elements, the eleven-membered carbocyclic ring is the most common, even though C_{11} rings are certainly not common. Surprisingly, the least common is the α,β-unsaturated δ-lactone with an isopropyl substituent at the β-position (Weihe and McMorris, 1978). However, once atranones D (**4**) and E (**5**) and the dolabellanes **8** and **9** were in hand, the biosynthetic relationship of atranones **1**–**3** to the dolabellane diterpenes was evident. Atranones A–C, F, and G (**1--3**, **6**, and **7**, respectively) appear to be derived from the atranone D and E series by way of a Baeyer–Villiger oxidation, a biosynthetic transformation more commonly observed in bacteria (Walsh and Chen, 1988; Wright et al., 1996) than in fungi (Minto and Townsend, 1997). The only example found in our literature search in natural products of the transformation of an α-methoxy-α,β-unsaturated enone ring into the corresponding α,β-unsaturated lactone ring was reported to have occurred in a plant-derived natural product (Felicio et al., 1986).

The highly functionalized 3,7-dioxabicyclo[3.3.0] octane-2-one ring system found in atranones A–C is also quite unusual. The only natural product examples of this system we have found reported are the plant-derived tenulins (Raffauf et al., 1975; Le Quesne et al., 1978) and eremantholides (Le Quesne et al., 1982; Takao et al., 1995). However, the 3,7-dioxabicyclo [3.3.0]octane-2-one system in these sesquiterpenes differs from that of the atranones by having an angular methyl at C-21 (atranone numbering) and by not being enol lactones. In fact, enol lactones, especially the non-conjugated types are also quite uncommon functional groups in natural products (Naito et al., 1991). There is however, one very interesting further connection between the atranones and the tenulins and eremantholides; the elaborated sequiterpenoid tenulins and eremantholides appear to arise from an alkylation at the α-position of the lactone by a neighboring acyl group (Fig. 4). In an analogous fashion, alkylation of the C-21 position in atranones F (**6**) and G (**7**) (following prior formal dehydration at the C-6/C-21 position) could lead to the atranone A–C series via an analogous pathway (Fig. 4).

The biosynthetic origin of the C-21/C-24 unit in the atranones is obscure; no other examples of alkylated dolabellanes have been reported (Rodríguez et al., 1998). However, there are derivatives of the cyathin diterpenes (Magnus and Shen, 1999) that are elaborated further through alkylation of C-6 (atranone numbering) by an appended xylose to give the erinacines E–G (Kawagishi et al., 1996) and the striatins (Hecht et al., 1978). Formally, the cyathin ring system is related to that of the dolabellanes by way of formation of a C-8/C-10 ring junction and migration of the 17-Me from C-8 to C-7 (atranone numbering) in the latter. The alkylation of the cyathin ring in the erinacines and striatins occurs at C-6, the same position alkylated in the dolabellanes that leads to the atranones. Recently, another example of a metabolite that appears to be a much elaborated dolabellane was isolated from *Hericium ramasoum* (Saito et al., 1998). A further interesting point about the atranones is that of the >50 isolates of *S. chartarum* grown in rice culture in our laboratory, we have not yet observed any that produce both the atranones and macrocyclic trichothecenes, which suggests that there are two chemotypes of *S. chartarum*. About

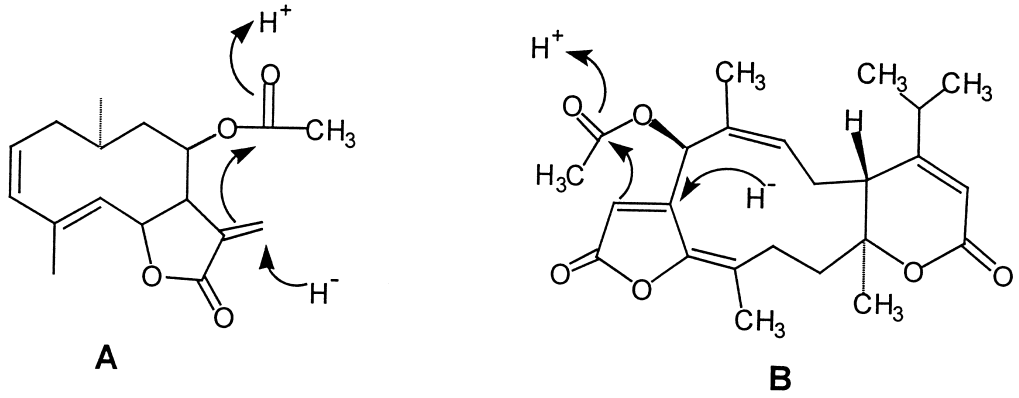

Fig. 4. Comparison of the proposed biogenesis of the eremantholides (**A**) (Le Quesne et al., 1978) and the atranones (**B**). The "H−" may be from a co-factor such as NADPH.

2/3 of the isolates are atranone producers while about 1/3 produce macrocyclic trichothecenes (Jarvis et al. 1998; Hinkley et al., 1999). A few (< 10%) do not appear to produce either of these classes of natural products, although all of the isolates of *S. chartarum* that we have examined produce the spirocyclic lactones and lactams (Jarvis et al., 1995).

Attempts to establish the absolute stereochemistry of these compounds has not yet been successful. Although the X-ray crystal structure data for atranone C (**3**) are quite good, the data could not be refined sufficiently to give an anomalous dispersion factor that would allow assignment of the absolute configuration of **3**. Rodríguez et al. (1998) have analyzed the literature on the dolabellanes and have concluded that the dolabellanes have antipodal structures depending upon the source. Thus, dolabellanes from mollusks, algae, and liverworts are antipodal to those isolated from the coelenterates (e.g. gogorians). The single example of a fungal-produced dolabellane (Jenny and Borschberg, 1995) has the same absolute stereochemistry at C-1/C-11 as is found in the dolabellanes produced by the coelenterates (Rodríguez et al., 1998). Thus, we have chosen to illustrate our compounds with this same stereochemistry, although there is no certainty on this point. Attempts to prepare heavy atom derivatives of several of the atranones with properties suitable for X-ray diffraction measurements have not yet been successful.

4. Experimental

Melting points were determined on a Lab Devices Mel-Temp and are uncorrected. Optical rotations were measured on a Jasco DIP-370 polarimeter. IR and UV spectra were recorded on Nicolet Magna-560 FT-IR and Beckmann DU-7 spectrophotometers, respectively. HRMS spectra were determined with a VG 7070E mass spectrometer. NMR spectra were recorded on Bruker DRX-400 and DRX-500 instruments with spectra referenced to the solvent resonance. Radial chromatography was performed on a Harrison Research 7924T Chromatotron.

S. chartarum, S-11 (Jarvis et al., 1986) was stored at −20°C on sterile dirt. Potato dextrose agar slants were prepared from spore suspensions thereof. Rice cultures were prepared by autoclaving rice (50 g, Uncle Ben's) with sterile distilled water (50 ml) in Erlenmeyer flasks (20×250-ml) at 122°C and 18.8 PSI for 20 min, and inoculating with a spore suspension. The flasks were held at room temperature for 4 weeks with hand-shaking every ~3 days; 850 g of the culture material was harvested. The rice was air dried, coarsely ground (1 s, coffee grinder), and 1.4 l of MeOH–$CHCl_3$ (1:1) added to the rice, and the mixture was sonicated in a bath for 1 h and left to stand overnight. The mixture was filtered, and the material re-extracted twice with MeOH–$CHCl_3$ (1 l, 1:1). The combined organic extracts were concentrated to 400 ml, water (500 ml) added, and the mixture extracted with $CHCl_3$ (4×150 ml). The extract was dried (Na_2SO_4), filtered, and the solvent removed by rotary evaporation to give the crude extract (16.0 g) which was triturated with hexane, reducing the mass to 11.5 g. The majority of the extract (7.5 g) was adsorbed onto polyethyleneimine silica gel (Jarvis, 1992) (PEI, 4 g) and the free flowing powder applied to a PEI column (100 g, 43×165 mm). Elution with increasing proportions of CH_2Cl_2 in hexane, then increasing amounts of MeOH in CH_2Cl_2 gave four fractions.

Fraction 1 (148.2 mg, eluted with hexane to 80% CH_2Cl_2-hexane) was applied to a 2 mm Chromatotron plate (eluting with 10% EtOAc in CH_2Cl_2) to yield atranones D (**4**) (14.7 mg) and E (**5**) (12.7 mg). A later fraction from the plate was purified twice more on 2 mm Chromatotron plates (10 and 20% EtOAc–CH_2Cl_2) to yield dolabellanes **8** (3.4 mg) and **9** (3.1 mg).

Fraction 2 (340 mg, eluted with 100% CH_2Cl_2) was applied to a 2 mm Chromatotron plate and eluted with EtOAc–hexane–MeOH (40:60:5) to give atranone B (**2**) (93.7 mg). A later fraction from the plate (163 mg) was

found to contain a 2:1 mixture of atranones A (**1**) and C (**3**). These were resolved by semipreparitive HPLC using the following conditions: RP C-18 column (Phenomenex, 10×250 mm); solvent MeOH:H_2O (isocratic, 2:5); flow, 3.5 ml/min; detection, UV 250 nm; retention time for **1** and **3**, 35.8 and 40.9 min, respectively.

Fraction 3 (66.4 mg, eluted with 1–20% MeOH–CH_2Cl_2) was loaded onto a 2 mm Chromatotron plate and eluted with EtOAc–hexane–MeOH (gradient from 1:9:0 to 70:30:1) to give atranones F (**6**) (4.0 mg) and G (**7**) (5.1 mg).

Physical and spectral data for atranones A–C (**1**–**3**) are given in Hinkley et al. (1999).

4.1. Atranone D (*4*)

Clear film; $[\alpha]_D^{20}$ +21 (*c* 0.70, $CHCl_3$); UV λ_{max}^{MeOH}(log ε) nm: 231 (4.17); IR $\nu_{max}^{CHCl_3}$ cm^{-1}: 3684, 3607, 3015, 2971, 2935, 1780, 1693, 1522, 1424, 1213; HREI–MS *m/z* 386.2451 $[M]^+$ ($C_{24}H_{34}O_4$ req. 386.2457); ^1H and ^{13}C NMR spectroscopic data are listed in Tables 1 and 2.

4.2. Atranone E (*5*)

Clear film; $[\alpha]_D^{20}$− 16 (*c* 0.75, $CHCl_3$); λ_{max}^{MeOH} (log ε) nm: 226 nm (4.10); IR $\nu_{max}^{CHCl_3}$ cm^{-1}: 3688, 3608, 3518, 2970, 2937, 2874, 1773, 1692, 1606, 1459, 1386, 1374, 1277, 1133, 1068; HREI–MS *m/z* 386.2447 $[M]^+$ ($C_{24}H_{34}O_4$ req. 386.2457); ^1H and ^{13}C NMR spectroscopic data are listed in Tables 1 and 2.

4.3. Atranone F (*6*)

Pale yellow film; $[\alpha]_D^{20}$ +24 (*c* 0.16, $CHCl_3$); λ_{max}^{MeOH} (log ε) nm: 237 (3.62) (shoulder with strong end absorption); IR $\nu_{max}^{CHCl_3}$ cm^{-1}: 369 (br), 2969, 2934, 1807, 1743, 1712, 1691, 1382, 1230, 1196, 1030, 991; HREI–MS *m/z* 432.2123 $[M]^+$ ($C_{24}H_{32}O_7$ req. 432.2148); ^1H and ^{13}C NMR spectroscopic data are listed in Tables 1 and 2.

4.4. Atranone G (*7*)

Pale yellow film; $[\alpha]_D^{20}$ +28 (*c* 0.2, $CHCl_3$); IR $\nu_{max}^{CHCl_3}$ cm^{-1}: 3390, 2963, 2930, 1808, 1743, 1718, 1374, 1260, 1233, 1092, 1023; HRFAB–MS *m/z* 463.2308 $[M+H]^+$ ($C_{25}H_{35}O_8$ req. 463.2232); ^1H and ^{13}C NMR spectroscopic data are listed in Tables 1 and 2.

4.5. (1S*, 6S*, 11S*)-6-Hydroxydolabella-3E, 7E, 12-trien-14-one (*8*)

Clear film; $[\alpha]_D^{20}$ −142 (*c* 0.23, $CHCl_3$); λ_{max}^{MeOH} (log ε) nm: 236 nm (3.94); IR $\nu_{max}^{CHCl_3}cm^{-1}$: 3684, 3608, 3017, 2970, 2933, 1690, 1654, 1521, 1423, 1214 (br); HREI–MS *m/z* 302.2246 $[M]^+$ ($C_{20}H_{30}O_2$ req. 302.2246); ^1H and ^{13}C NMR spectroscopic data are listed in Table 3.

4.6. (1S*, 3R*, 4R*, 6S*, 11S*)-3,4-Epoxy-6-hydroxydolabella-7E, 12-dien-14-one (*9*)

Clear film; $[\alpha]_D^{20}$ −77.3 (c 0.21, $CHCl_3$); λ_{max}^{MeOH} (log ε) nm: 235 nm (3.95); IR $\nu_{max}^{CHCl_3}$ cm^{-1}: 3683, 3608, 3015, 2971, 2934, 1696, 1522, 1424, 1209 (br), 929; HREI–MS *m/z* 318.2198 $[M]^+$ ($C_{20}H_{30}O_3$ req. 318.2206); ^1H and ^{13}C NMR spectroscopic data are listed in Table 3.

4.7. Single-crystal X-ray diffraction analysis of atranone C (*3*)

A colorless crystalline parallelepiped, obtained by diffusing hexane into an ethyl acetate solution of atranone C, with dimensions 0.500×0.163×0.102 mm^3 was placed and optically centered on the Bruker SMART CCD system at −100°C. The initial unit cell was indexed using a least-squares analysis of a random set of reflections collected from three series of 0.3° wide ω scans (25 frames/series) that were well distributed in reciprocal space. Data frames were collected [MoK_α] with 0.3° wide ω scans, 40 s/frame, 606 frames per series, 5 complete series and an additional 60 frames of the first series for decay purposes, a crystal to detector distance of 4.94 cm, providing a complete sphere of data to $2\theta_{max}$ = 55.0°. A total of 33555 reflections were collected and corrected for Lorentz and polarization effects and absorption using Blessing's method as incorporated into the program SADABS (Blessing, 1995; Sheldrick, 1996) with 5091 unique [R(int) = 0.0252].

All crystallographic calculations were performed on a personal computer (PC) with dual Pentium 450 MHz processors and 256 MB of extended memory. The SHELXTL (Sheldrick, 1994) program package was implemented, XPREP, to determine the probable space group and set up the initial files. System symmetry and systematic absences indicated the unique non-centrosymmetric orthorhombic space group $P2_12_12_1$ (no. 19) with intensity statistics clearly in agreement. The structure was determined by direct methods with the successful location of nearly all non-hydrogen atoms using the program XS (Sheldrick, 1990). The structure was refined with XL (Sheldrick, 1993). After the initial refinement difference-Fourier cycle, additional non-hydrogen atoms were located and input. After one of these refinement difference-Fourier cycles, all of the non-hydrogen atoms were refined isotropically, then anisotropically. Hydrogen atoms were initially placed in calculated positions but later allowed to refine freely (xyzU). The final structure was refined to convergence [$\Delta/\sigma \leqslant 0.001$] with R(F) = 3.39%, wR($F^2$) = 8.22%, GOF = 1.047 for all 5091 unique reflections [R(F) = 3.01%, wR(F^2) = 8.03% for those 4603 data with Fo > 4σ (Fo)]. A final difference-Fourier map was featureless, with the largest peak $|\Delta\rho| \leqslant 0.24$ $eÅ^{-3}$, indicating that the structure is both correct and complete.

The absolute structure parameter was also refined, Flack(x) = 1.0(6), indicating that the absolute structure cannot be determined reliably due to the lack of any atoms present with significant anomalous dispersion (Flack, 1983).

The function minimized during the full-matrix least-squares refinement was $\Sigma w(Fo^2\text{-}Fc^2)$ where $w = 1/[\sigma^2(Fo^2) + (0.0571*P)^2 + 0.0*P]$ and $P = (\max(Fo^2,0) + 2*Fc^2)/3$. An empirical correction for extinction was also applied to the data in the form $(Fc^2,\text{corr}) = k[1 + 0.001 * x * Fc^2 * \lambda^3/\sin(2\theta)]^{(-1/4)}$ where $k = 0.41425$ is the overall scale factor. The value determined for x was 0.0020(7).

5. Supporting information available

X-ray crystal data are deposited at the Cambridge Crystallographic Centre (www.ccdc.cam.ac.uk).

Acknowledgements

This work was supported by the Center for Indoor Air Research (contract 05–98). The authors wish to express their thanks to Professor George Bean for growing the rice culture, Caroline Ladd for collecting HRMS data, Dr. Hermon Ammon for providing access to modeling software, and the technical support of Kim Dudley.

References

Asakawa, Y., 1995. Chemical constituents of the bryophytes. Progress in the chemistry of natural products 65, 219–226.

Blessing, R.H., 1995. An empirical correction for absorption anisotropy. Acta Crystallographica A51, 33–38.

Corey, E.J., Kania, R.S., 1998. Concise total synthesis of (±)-dolabellatrienone via a dianion-accelerated oxy-Cope rearrangement. Tetrahedron Letters 39 (8), 741–744.

Dearborn, D.G., Yike, I., Sorenson, W.G., Miller, M.J., Etzel, R.A., 1999. Overview of investigations into pulmonary hemorrhage among infants in Cleveland, Ohio. Environmental Health Perspectives 107 (6) (Supplement 3), 495–499.

Etzel, R.A., Montana, E., Sorenson, W.G., Kullman, G.J., Allen, T.M., Olson, D.R., Jarvis, B.B., Miller, J.D., Dearborn, D.G., 1998. Acute pulmonary hemorrhage in infants associated with exposure to *Stachybotrys atra* and other fungi. Archives of Pediatric and Adolescent Medicine 152 (8), 757–762.

Felicio, J.D., Motidome, M., Yoshida, M., Gottlieb, O.R., 1986. Further neolignans from *Ocotea aciphylla*. Phytochemistry 25 (7), 1707–1710.

Flack, H.D., 1983. On enantiomorph-polarity estimation. Acta Crystallographica A39, 876–881.

Forgacs, J., 1972. Stachybotryotoxicosis. In: Kadis, S., Ceigler, A., Ajl, S.J. (Eds.), Microbial toxins, Vol. VIII. Academic Press, New York, pp. 95–128.

Hecht, H.-J., Höfle, G., Steglich, W., Anke, T., Oberwinkler, F. 1978. Striatin A, B, and C: novel diterpenoid antibiotics from *Cyathus striatus*; X-ray crystal structure of striatin A. Journal of the Chemical Society Chemical Communications 665–666.

Hinkley, S.F., Jiang, J., Mazzola, E.P., Jarvis, B.B., 1999. Atranones: Novel diterpenoids from the toxigenic mold *Stachybotrys atra*. Tetrahedron Letters 40 (14), 2725–2728.

Hintikka, E.-L., 1978. Human stachybotryotoxicosis. In: Wyllie, T.D., Morehouse, L.G. (Eds.), *Mycotoxic Fungi Mycotoxins, Mycotoxicoses*, Vol. 3. Marcel Dekker, New York, pp. 87–89.

Jarvis, B.B., 1991. Macrocyclic trichothecenes. In: Sharma, R.P., Salunkhe, D.K. (Eds.), Mycotoxins and Phytoalexins in Human and Animal Health. CRC Press, Boca Raton, FL, pp. 361–421.

Jarvis, B.B., 1992. Macrocyclic trichothecenes from Brazilian *Baccharis* species: from microanalysis to large scale isolation. Phytochemical Analysis 3 (6), 241–249.

Jarvis, B.B., Lee, Y.-W., Yatawara, S.N., Cömezoglu, C.S., 1986. Trichothecenes produced by *Stachybotrys atra* from Eastern Europe. Applied and Environmental Microbiology 51 (5), 915–918.

Jarvis, B.B., Salemme, J., Morais, A., 1995. *Stachybotrys* toxins. 1. Natural Toxins 3 (1), 10–16.

Jarvis, B.B., Sorenson, W.G., Hintikka, E.-L., Nikulin, M., Zhou, Y., Jiang, J., Wang, S., Hinkley, S., Etzel, R.A., Dearborn, D., 1998. Study of toxin production by isolates of *Stachybotrys chartarum* and *Memnoniella echinata* isolated during a study of pulmonary hemosiderosis in infants. Applied and Environmental Microbiology 64 (10), 3620–3625.

Jenny, L., Borschberg, H.-J., 1995. Synthesis of the dolabellane diterpene hydrocarbon (±)-δ-araneosene. Helvetica Chimica Acta 78 (3), 715–731.

Jong, S.C., Davis, E.E., 1976. Contribution to the knowledge of *Stachybotrys* and *Memnoniella* in culture. Mycotaxon 3 (3), 409–485.

Kawagishi, H. et al., 1996. Erinacines E, F, and G, stimulators of nerve growth factor (NGF)-synthesis, from the mycelia of *Hericum erinaceum*. Tetrahedron Letters 37 (41), 7399–7402.

Le Quesne, P., Levery, S.B., Menachery, M.D., Brennan, T.F., Raffaut, R.F., 1978. Antitumour plants. Part 6. Novel modified germacranolides and other constituents of *Eremanthus elaeagnus* Schultz-Bip (*Compositae*). Journal of the Chemical Society Perkin I 12, 1572–1580.

Le Quesne, P., Menachery, M.D., Pastore, M.P., Kelly, C.J., Brennan, T.F., Onan, K.D., Raffaut, R.F., 1982. Antitumor plants. 12. Further sesquiterpenoid constituents of *Lychnophora affinis* Gardn. (*Compositae*). X-ray structure analysis of lychnophorolide A. The Journal of Organic Chemistry 47 (8), 1519–1521.

Magnus, P., Shen, L., 1999. Stereoselective synthesis of the "cyathin" diterpene skeleton via an intramolecular pyrylium ylide-alkene cyclization. Tetrahedron 55 (12), 3553–3560.

Minto, R.E., Townsend, C.A., 1997. Enzymology and molecular biology of aflatoxin biosynthesis. Chemical Reviews 97 (7), 2537–2555.

Naito, T., Katsuhara, T., Niitsu, K., Ikeya, Y., Okada, M., Mitsuhashi, H., 1991. Phthalide dimers from *Ligusticum chuangxiong* Hort. Heterocycles 32 (12), 2433–2442.

Neuhaus, D., Williamson, M.P., 1989. The Nuclear Overhauser Effect in Structural and Conformational Analysis. VCH Publishers, New York, pp. 97–100; 358–359.

Raffauf, R.F., Huang, P.-K., Le Quesne, P.W., Levery, S.B., Brennan, T.F., 1975. Eremantholide A, a novel tumor-inhibiting compound from *Eremanthus elaeagnus* Schultz-Bip (*Compositae*). The Journal of the American Chemical Society 97 (23), 6884–6886.

Rodríguez, A.D., González, E., Ramírez, C., 1998. The structural chemistry, reactivity, and total synthesis of dolabellane diterpenes. Tetrahedron 54 (39), 11683–11729.

Saito, T., Aoki, F., Hirai, H., Inagaki, Y., Matsunaga, Y., Sakakibara, T., Sakemi, S., Suzuki, Y., Watanabe, S., Suga, O., Sujaku, T., Smogowicz, A.A., Truesdell, S.J., Wong, J.W., Nagahisa, A., Kojima, Y., Kojima, N., 1998. Erinacine E as a kappa opioidreceptor agonist and its new analogs from a Basidiomycete, *Hericium ramosum*. The Journal of Antibiotics 51 (11), 983–990.

Sanders, J.K.M., Mersh, J.D., 1982. Nuclear magnetic double resonance; the use of difference spectroscopy. Progress in Nuclear Magnetic Resonance Spectroscopy 15 (part 6), 353–400.

Sheldrick, G.M., 1990. Phase annealing in SHELX-90: Direct methods for larger structures. Acta Crystallographica A46, 467–473.

Sheldrick, G. M., 1993. Shelxl93 program for the refinement of crystal structures. University of Göttingen, Göttingen, Germany.

Sheldrick, G. M., 1994. SHELXTL/PC. Version 5.03. Siemens Analytical X-ray Instruments Inc., Madison, Wisconsin, USA.

Sheldrick, G. M. 1996. SADABS Siemens area detector absorption correction. Universität Göttingen, Göttingen, Germany.

Shin, J., Fenical, W., 1991. Structures and reactivities of new dolabellane diterpenoids from the Caribbean gorgonian *Eunicea iaciniata*. The Journal of Organic Chemistry 56 (10), 3392–3398.

Takao, K.-i., Ochiai, H., Yoshida, K.-i., Hashizuka, T., Koshimura, H., Tadano, K.-i., Ogawa, S., 1995. Novel total synthesis of (+)-ermantholide A.. The Journal of Organic Chemistry 60 (25), 8179–8193.

Walsh, C.T., Chen, Y.-C., 1988. Enzymic Baeyer–Villiger oxidations by flavin-dependent monooxygenases. Angewandte Chemie International Edition in English 27 (2), 333–343.

Weihe, G.R., McMorris, T.C., 1978. Stereoselective synthesis of 23-deoxyantheridiol. The Journal of Organic Chemistry 43 (20), 3942–3946.

Wright, J.L.C., Hu, T., McLachlan, J.L., Needham, J., Walter, J.A., 1996. Biosynthesis of DTX-4: Confirmation of a polyketide pathway, proof of a Baeyer–Villiger oxidation step, and evidence for an unusual carbon deletion process. The Journal of the American Chemical Society 118 (36), 8757–8758.